

Article

Degradation of Oxytetracycline by Persulfate Activation Using a Magnetic Separable Iron Oxide Catalyst Derived from Hand-Warmer Waste

Youn-Jun Lee ¹, Chang-Gu Lee ^{1,*}, Seong-Jik Park ²  and Eun Hea Jho ^{3,*} 

¹ Department of Environmental and Safety Engineering, Ajou University, Suwon 16499, Korea; duswnss@ajou.ac.kr

² Department of Bioresources and Rural Systems Engineering, Hankyong National University, Anseong 17579, Korea; parkseongjik@hknu.ac.kr

³ Department of Agricultural and Biological Chemistry, Chonnam National University, Gwangju 61186, Korea

* Correspondence: changgu@ajou.ac.kr (C.-G.L.); ejho001@chonnam.ac.kr (E.H.J.); Tel.: +82-31-219-2405 (C.-G.L.); +82-62-530-2134 (E.H.J.)

Abstract: Oxytetracycline (OTC) is a tetracycline antibiotic that is widely used in the drug therapy and livestock industry and may threaten human health and ecosystems when released into the environment. In this study, a catalyst was prepared from hand-warmer waste using a simple magnetic separation method. The prepared hand-warmer waste catalyst (HWWC) was used as a persulfate (PS) activator for OTC removal. Characterization methods, such as X-ray diffraction and scanning electron microscopy–energy dispersive X-ray spectrometry, were used to investigate the crystal structure, surface morphology, and weight ratios of the elements in the HWWC. The degradation efficiency of OTC in the presence of the catalyst and PS was studied, and the radical generation mechanism of the catalyst was investigated. The removal ratio of OTC by PS activation was greater than 99% for a reaction time of 24 min at a pH of 6. The effects of the HWWC dosage, PS concentration, and solution pH on OTC degradation were also investigated. The reuse test revealed that HWWC can be reused for eight cycles with great stability. These results suggest that PS activation using hand-warmer waste can be an efficient strategy for the degradation of antibiotics.

Keywords: antibiotics; persulfate activation; hand-warmer waste; magnetic separable iron oxide catalyst; Fenton-like reaction



Citation: Lee, Y.-J.; Lee, C.-G.; Park, S.-J.; Jho, E.H. Degradation of Oxytetracycline by Persulfate Activation Using a Magnetic Separable Iron Oxide Catalyst Derived from Hand-Warmer Waste. *Appl. Sci.* **2021**, *11*, 10447. <https://doi.org/10.3390/app112110447>

Academic Editor: Rajender S. Varma

Received: 4 October 2021

Accepted: 5 November 2021

Published: 7 November 2021

Publisher's Note: MDPI stays neutral with regard to jurisdictional claims in published maps and institutional affiliations.



Copyright: © 2021 by the authors. Licensee MDPI, Basel, Switzerland. This article is an open access article distributed under the terms and conditions of the Creative Commons Attribution (CC BY) license (<https://creativecommons.org/licenses/by/4.0/>).

1. Introduction

The amount of antibiotics released into the environment is increasing owing to the lack of appropriate disposal methods and strict control measures, which threaten human health and the ecosystem [1,2]. Oxytetracycline (OTC), an antibiotic, is widely used as an antimicrobial agent and growth factor in drug therapy and the livestock industry [3,4]. Approximately 70% of OTC leaves organisms via urine and feces without undergoing metabolism because of its poor absorption [5]. Therefore, OTC has been detected in various environments, such as aquatic systems, soil, and sediments [6–8]. In aquatic environments, several studies have reported that OTC has been detected in river water [9] and in the influent and effluent of a wastewater treatment plant [10–13]. However, it is difficult to degrade the released OTC in water using conventional wastewater treatment processes [14]. Therefore, effective treatment of OTC in water is a problem that needs to be solved urgently.

Sulfate radicals ($\text{SO}_4^{\bullet-}$) and hydroxyl radicals (HO^{\bullet}) are widely used reactive radical species in wastewater treatment because of their high oxidizing capabilities [15]. Generally, activating peroxides such as persulfate (PS), peroxymonosulfate, and hydrogen peroxide or photocatalytic processes can generate these radical species [16]. Among the above-mentioned peroxides, PS is much cheaper and easier to activate owing to its low band energy (140 kJ/mol) [17,18], PS has attracted attention as an oxidant for degrading various

pollutants [19,20]. Catalysts such as metal-containing oxides and transition metals have been used to activate PS because they are energy-free and economic [21–23]. Moreover, research on the reuse of waste containing metal elements such as Fe as a PS activator has been conducted [16,24,25].

Disposable hand warmers are widely used to keep oneself warm; thus, the demand for hand warmers greatly increases in winter. After exposure to air, the materials in the hand warmer pocket react and release heat for a period of time. The spent hand warmer is then discarded, which can adversely affect the environment and lead to wastage of resources [26], recycling or reusing the spent hand warmer is needed to reduce environmental pollution. Hand-warmer waste generally contains iron oxide (Fe_2O_3) particles. Therefore, reusing hand-warmer waste for the activation of PS can be an environmentally friendly and cost-saving technique. To the best of our knowledge, this study is the first to recycle hand-warmer waste as a catalyst for PS activation.

In this study, a hand-warmer waste catalyst (HWWC) was prepared by a simple magnetic separation method and used as a PS activator for OTC degradation. The surface morphology and crystal structure of the prepared HWWC were investigated. The effects of the catalyst dosage, PS concentration, and pH on the degradation of OTC were studied. In addition, the stability of the catalyst was evaluated by conducting a reuse test.

2. Materials and Methods

2.1. Chemical and Materials

A hand warmer was obtained from DABONG Industrial Co., Ltd. (Seoul, Korea). Oxytetracycline hydrochloride ($\text{C}_{22}\text{H}_{24}\text{N}_2\text{O}_9 \cdot \text{HCl} \geq 97.5\%$) was purchased from Sigma-Aldrich Co., Ltd. (Burlington, MA, USA). Sodium phosphate monobasic anhydrous ($\text{NaH}_2\text{PO}_4 \geq 98\%$), sodium phosphate dibasic anhydrous ($\text{Na}_2\text{HPO}_4 \geq 99.0\%$), sodium hydroxide ($\text{NaOH} \geq 98.0\%$), hydrogen chloride ($\text{HCl} \geq 35.0\text{--}37.0\%$), and acetonitrile (ACN) ($\text{CH}_3\text{CN} \geq 99.9\%$) were purchased from Samchun Pure Chemical Co., Ltd. (Pyeongtaek-si, Korea). Sodium persulfate ($\text{Na}_2\text{S}_2\text{O}_8 \geq 98\%$) was purchased from Junsei Chemical Co., Ltd. (Tokyo, Japan). Deionized (DI) water with a resistivity of $18.2 \text{ M}\Omega/\text{cm}$ (Millipore, Darmstadt, Germany) was used to prepare the solutions.

2.2. Catalyst Preparation

HWWC was prepared using a simple magnetic separation method. After a disposable hand warmer was exposed to air for 36 h, 10 g of the contents inside the hand warmer were placed in 1 L of DI water. The Fe_2O_3 in the DI water was then magnetically separated. The separation process was repeated three times, and the obtained solid was dried in an oven at 80°C for 24 h. The dried solid was ground for further experiments.

2.3. Experimental Procedure

The OTC degradation experiments were initiated by adding 1 mM PS to 50 mL of the solution containing 20 μM OTC and 0.2 g/L HWWC. The reaction was conducted in a shaking incubator at 150 rpm and 25°C . The pH of the solution was adjusted to 3, 4, 6, and 8 using 0.1 M NaOH and 0.1 M HCl and analyzed using a pH meter (Orion Star A211, Thermo, Waltham, MA, USA). To perform the reuse test, the catalyst was magnetically separated after each reaction cycle.

2.4. Analytical Method

The OTC concentration was measured using a YL 9100 HPLC system (Youngin Chromass, Anyang, Korea) with a YL 9120 UV/Vis detector and YL 9150 autosampler. A YL C18-4D column ($4.6 \text{ mm} \times 150 \text{ mm}$, $5 \mu\text{m}$) was used to separate methanol, ACN, and 10 mM phosphate buffer (pH of 7) (15:15:70). The mobile phase was isocratically eluted at a flow rate of 1.0 mL/min. The column temperature was 35°C , and OTC was detected at 260 nm.

2.5. Characterization

The surface morphology and elemental contents of the HWWC were observed using a scanning electron microscope-energy dispersive X-ray spectrometer (SEM-EDS) (JSM-7900F, JEOL, Tokyo, Japan). The X-ray diffraction (XRD) pattern of the catalyst was analyzed using an XRD system (D/max-2500V, Rigaku, Tokyo, Japan). The point of zero charge (pH_{pzc}) of HWWC was determined by titration method with slight modification [27]. HWWC (0.04 g) was suspended in 20 mL of 0.01 M NaNO_3 for 24 h. Then the pH of solution was adjusted using 0.1 M HNO_3 or NaOH solution. To reach the equilibrium, the solution was agitated for 1 h, then the $\text{pH}_{\text{initial}}$ was measured. After measuring the $\text{pH}_{\text{initial}}$, 0.6 g of NaNO_3 was added to the suspension. After 3 h, the pH_{final} of the solution was measured. The pH_{pzc} value was determined as ΔpH ($\text{pH}_{\text{final}} - \text{pH}_{\text{initial}}$) was 0 when plotting ΔpH against pH_{final} . As shown in Figure 1a, pH_{pzc} of HWWC was 7.4. The magnetic property of HWWC was measured using vibrating sample magnetometer (VSM) (Model 7404, Lake shore cryotronics, Westerville, OH, USA).

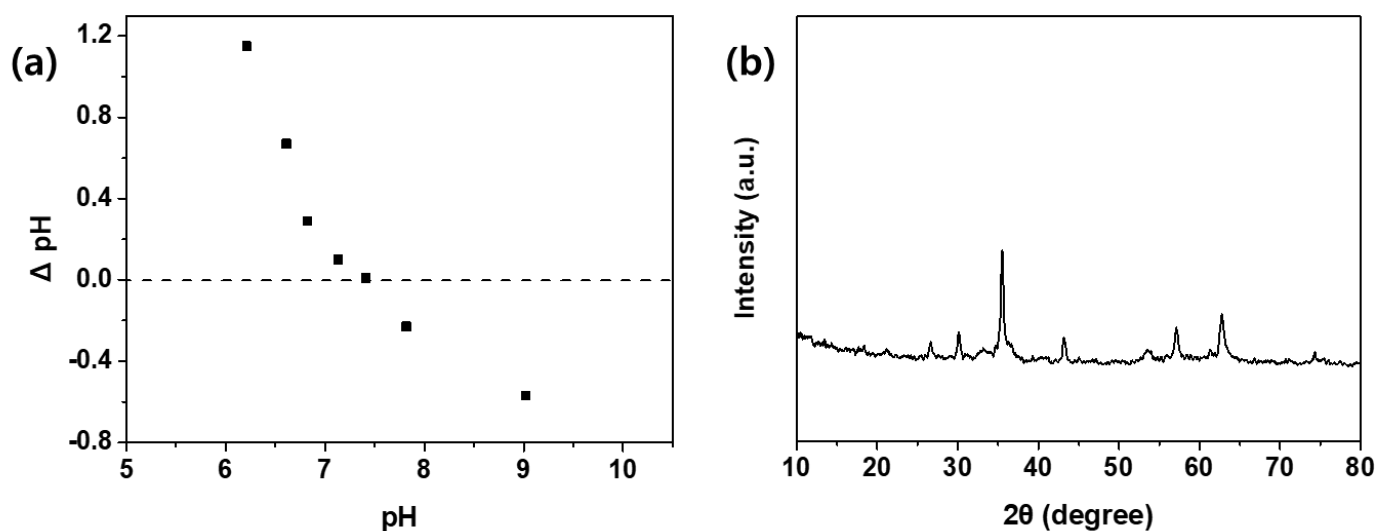


Figure 1. (a) pH_{pzc} measurement and (b) X-ray diffraction pattern of prepared hand-warmer waste catalyst.

3. Results and Discussion

3.1. Crystal Structure, Surface Morphology, and Magnetic Properties of HWWC

Figure 1b shows the XRD patterns of the prepared HWWC. The strongest peak observed at approximately $2\theta = 35.58^\circ$ indicated a reduction in the (119) diffraction of $\gamma\text{-Fe}_2\text{O}_3$ [28]. The peaks observed at approximately 30.08° , 43.16° , 57.16° , and 62.80° corresponding to (205), (0012), (1115), and (4012) were also in good agreement with those of $\gamma\text{-Fe}_2\text{O}_3$ [28,29]. Other impurity peaks at approximately 33.30° , 54.10° , and 63.40° agreed with $\alpha\text{-Fe}_2\text{O}_3$ [30]. These results indicated that the magnetically separated HWWC was a mixture mainly consisting of $\gamma\text{-Fe}_2\text{O}_3$ and $\alpha\text{-Fe}_2\text{O}_3$.

Figure 2 shows the SEM images and EDS spectra of the HWWC particles. The morphology of the particles was approximately spherical (Figure 2a). Based on the elemental analysis ($\text{O} = 32.23\%$, $\text{Fe} = 66.98\%$) (Figure 2b), it was determined that the sample mainly consisted of Fe and O, therefore confirming that the produced powder was Fe_2O_3 , which agreed with the XRD results.

Figure 3 shows the VSM analysis result of the HWWC particles. The saturation magnetization of the HWWC was determined to be 34.14 emu/g , which was sufficient ($>16.3 \text{ emu/g}$) for it to be magnetically recovered from solution using a conventional magnet [31,32]. Thus, HWWC can be easily recovered from water through magnetic separation and reused.

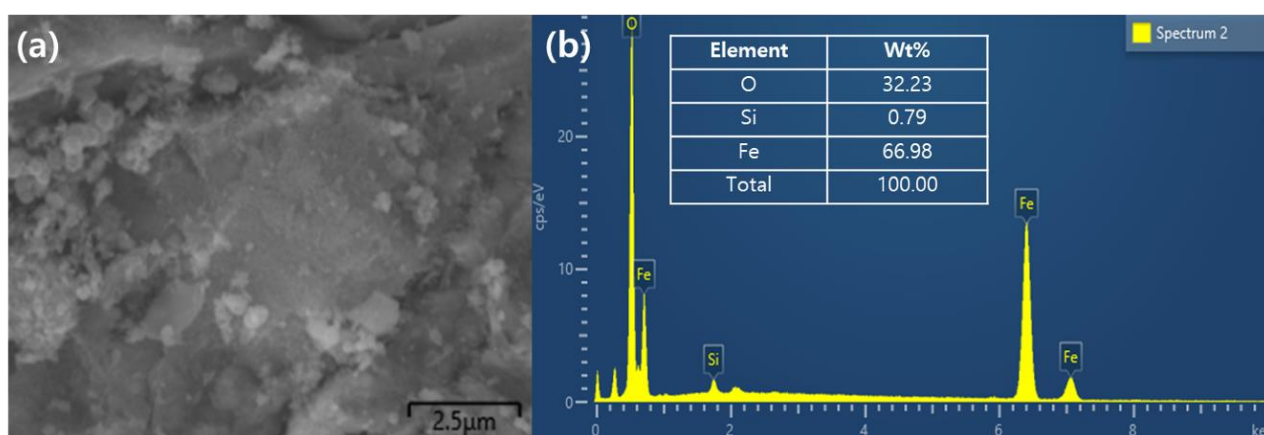


Figure 2. (a) Scanning electron microscope image and (b) energy dispersive X-ray spectrometer result of the prepared hand-warmer waste catalyst.

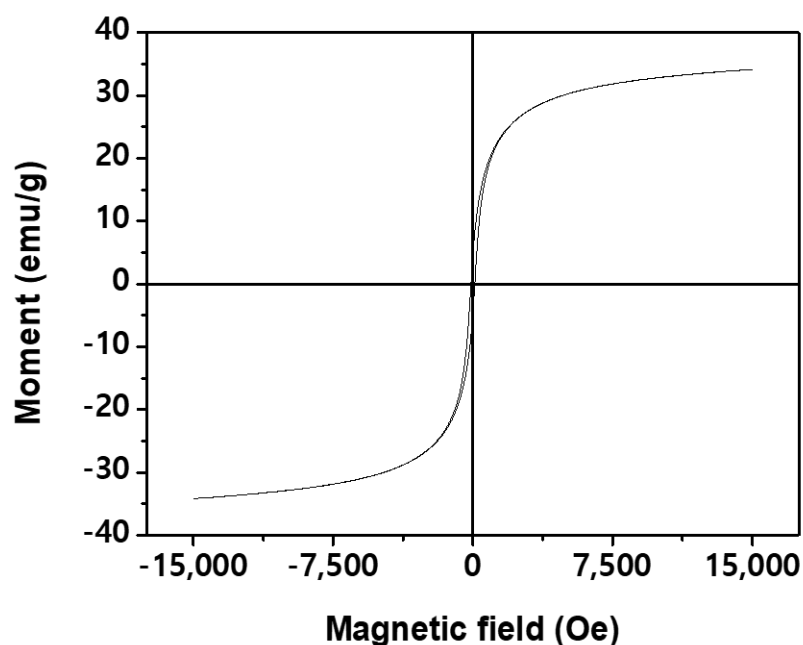
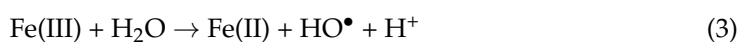
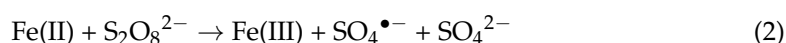
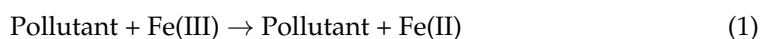


Figure 3. Vibrating sample magnetometer (VSM) analysis result of HWWC.

3.2. Control Experiments

Figure 4 shows the removal of OTC under different experimental conditions. OTC was removed when both PS and HWWC were present. The degradation efficiency of OTC by PS activation was greater than 99% in 24 min, and the estimated pseudo first-order rate constant (k) was $0.21 \pm 0.03 \text{ min}^{-1}$. This removal rate was comparable to OTC degradation through the Fenton process using $\text{H}_2\text{O}_2/\text{Fe}^{2+}$ ($k_{\text{app}} = 0.068\text{--}0.213 \text{ min}^{-1}$) [33], which indicates that the PS activation process using HWWC can be a promising technique for removing antibiotics from water. The removal rate of OTC in the presence of PS and HWWC in 24 min was low (<6.0%). The degradation mechanism of OTC by PS activation can be expressed by the following equations (Equations (1)–(5)) [34]:



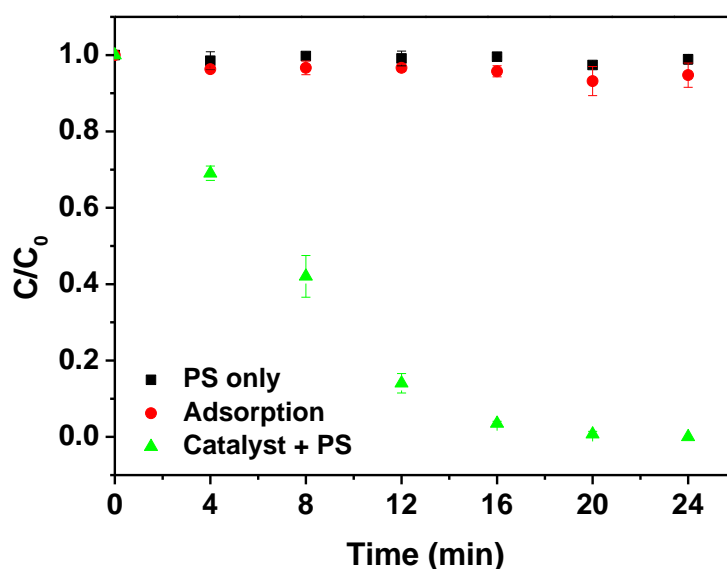
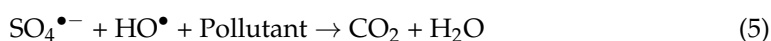
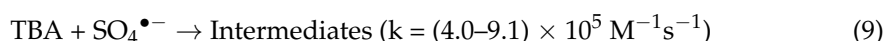
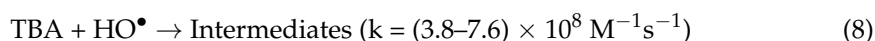
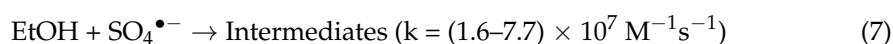
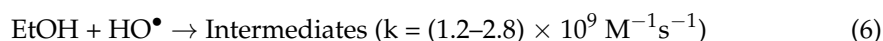


Figure 4. Control experiment for oxytetracycline (OTC) degradation ($[\text{PS}]_0 = 1 \text{ mM}$, $[\text{OTC}]_0 = 20 \text{ }\mu\text{M}$, $[\text{HWWC}]_0 = 0.2 \text{ g/L}$, $\text{pH} = 6$). PS: persulfate; HWWC: hand-warmer waste catalyst.

The electrons could be transferred to Fe(III) when the pollutant was adsorbed onto the Fe_2O_3 surface (Equation (1)). Therefore, a Fenton-like reaction occurred between $\text{S}_2\text{O}_8^{2-}$ and Fe(II) at the surface of Fe_2O_3 , therefore generating $\text{SO}_4^{\bullet-}$ and reforming Fe(III) (Equation (2)). HO^\bullet also might have been formed by this reaction and contributed to pollutant degradation (Equations (3)–(5)) [35–37]. Therefore, the pollutant could be degraded by the generated surface-adsorbed radicals ($\text{SO}_4^{\bullet-}$ and HO^\bullet) that might diffuse into the aqueous solution (Equation (5)) [34].

Figure 5 shows the effect of two radical scavengers, ethanol (EtOH) and *t*-butanol (TBA), on the degradation of OTC. According to equations (Equations (6)–(9)) [38], the reaction rate of EtOH and HO^\bullet is 50 times faster than that of EtOH and $\text{SO}_4^{\bullet-}$, while TBA reacts with HO^\bullet almost 1000 times faster than that with $\text{SO}_4^{\bullet-}$. From the results, the oxidation of OTC was significantly reduced with the addition of TBA and EtOH, suggesting that EtOH can effectively inhibit the oxidation efficiency. In addition, compared with EtOH, the removal rate of OTC was found to be lower in the presence of TBA, which demonstrates that a small amount of $\text{SO}_4^{\bullet-}$ remaining in the solution can still decompose OTC. Thus, it can be concluded that $\text{SO}_4^{\bullet-}$ is the dominant oxidizing species in the OTC degradation process by persulfate activation using HWWC catalysts.



3.3. Effects of HWWC Dosage and PS Concentration on OTC Degradation

The catalyst dosage and PS concentration are important factors in pollutant degradation. Therefore, degradation experiments with various HWWC dosages (0.05, 0.20, and 0.40 g/L) and PS concentrations (0.5, 1.0, and 2.0 mM) were investigated. As shown in Figure 6, the degradation efficiency of OTC increased in proportion to the HWWC dosage and PS concentration. The k value increased from $0.02 \pm 0.00 \text{ min}^{-1}$ to $0.14 \pm 0.02 \text{ min}^{-1}$ and increased from $0.09 \pm 0.01 \text{ min}^{-1}$ to $0.12 \pm 0.01 \text{ min}^{-1}$ when the HWWC dosage

and PS concentration increased, respectively. HWWC and PS were the activator and source of reactive radical species, respectively. Thus, their increase could promote OTC degradation [39].

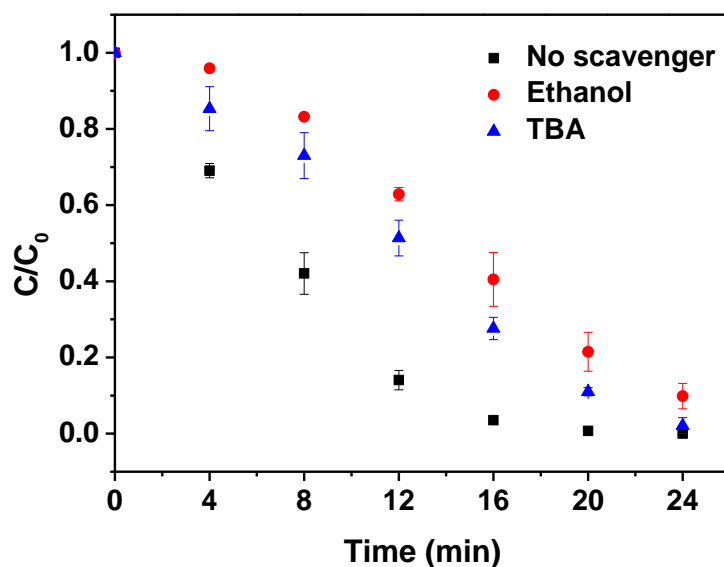


Figure 5. Oxytetracycline (OTC) degradation in the presence of scavengers ($[OTC]_0 = 20 \mu\text{M}$, $[PS]_0 = 1 \text{ mM}$, $[HWWC]_0 = 0.2 \text{ g/L}$, $[\text{scavenger}]_0 = 10 \text{ mg/L}$, $\text{pH} = 6$). PS: persulfate; HWWC: hand-warmer waste catalyst.

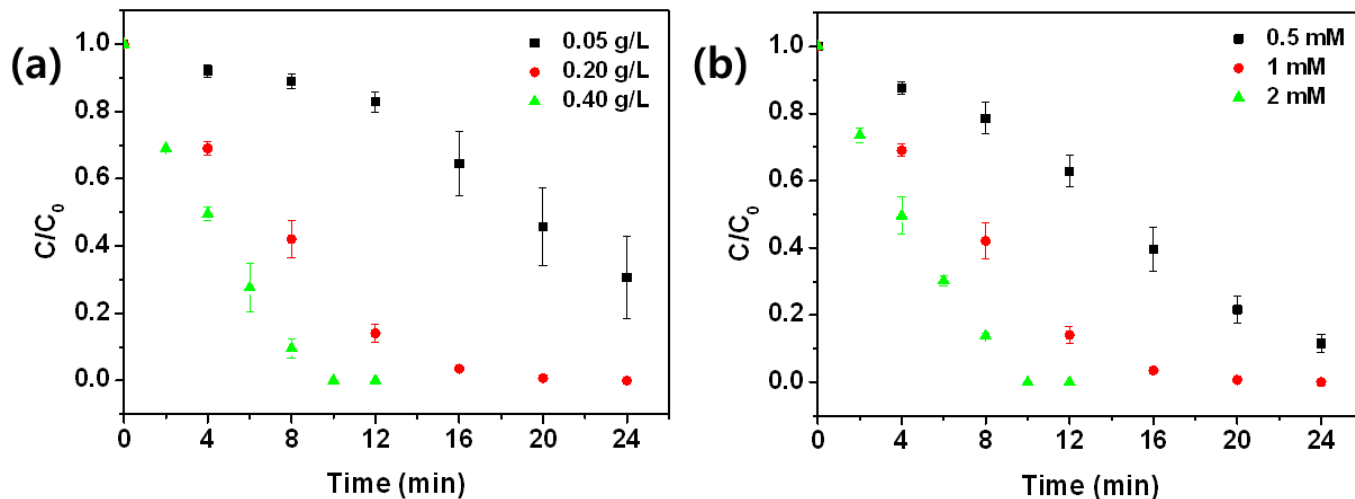


Figure 6. Oxytetracycline (OTC) degradation with (a) different catalyst dosages and (b) different persulfate concentrations ($[OTC]_0 = 20 \mu\text{M}$).

3.4. Effects of pH on OTC Degradation

In heterogeneous PS activation, the initial pH has a significant influence on the degradation of pollutants [40]. Therefore, the degradation efficiency at various solution pH conditions (3, 4, 6, and 8) was investigated (Figure 7). As shown in Figure 5, the removal ratio of OTC at 4 min was $70.8 \pm 7.0\%$, $70.7 \pm 0.8\%$, $31.0 \pm 1.9\%$, and $28.6 \pm 0.9\%$ at a pH of 3, 4, 6, and 8, respectively. The degradation performance at a pH of 3 and 4 showed no significant change, but the efficiency significantly decreased when the solution pH increased from 4 to 8, therefore implying that acidic conditions were more favorable for the degradation of OTC by heterogeneous PS activation. This result was observed because the surface properties of the catalyst and the lifetimes of the generated radical species changed

as the solution pH changed. When the point of zero charge of the catalyst was higher than the solution pH, the surface of the catalyst displayed a positive charge; thus, it could adsorb more $\text{SO}_4^{\bullet-}$ [41]. In addition, the lifetimes of HO^\bullet and $\text{SO}_4^{\bullet-}$ decreased under alkaline conditions; thus, the radical species that diffused into the bulk phase might have been insufficient for further degradation [42].

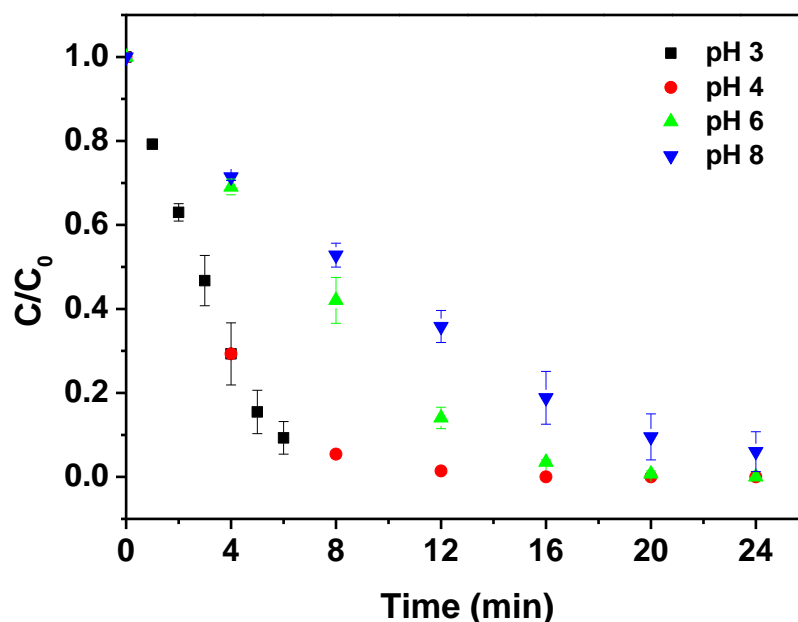


Figure 7. Oxytetracycline (OTC) degradation efficiency with different pH conditions ($[\text{PS}]_0 = 1 \text{ mM}$, $[\text{OTC}]_0 = 20 \text{ }\mu\text{M}$, $[\text{HWWC}]_0 = 0.2 \text{ g/L}$). PS: persulfate; HWWC: hand-warmer waste catalyst.

3.5. Applicability of HWWC

The stability of the catalyst is an important index for practical applications in wastewater treatment. Therefore, sequential OTC degradation experiments were performed to test the reusability of the catalyst (Figure 8a). The reaction was conducted for 24 min, after which the HWWC was recovered using an external magnet. The degradation performance of the HWWC did not significantly decrease after eight repeat experiments with a final degradation efficiency of 92.7%. This result indicated that the catalyst exhibited excellent regeneration performance and stability. Since the actual environmental water contains a large amount of organic and inorganic compounds, the activity of $\text{SO}_4^{\bullet-}$ and HO^\bullet may be reduced. Therefore, it is necessary to investigate the effect of radical scavengers of these organic and inorganic compounds. Chloride ion (Cl^-), one of the representative inorganic compounds present in large amounts in environmental water, can reduce degradation efficiency by the following equations (Equations (10)–(11)) [38,43]. In the present condition, however, the effect of chloride ion ($[\text{Cl}^-]_0 = 10 \text{ mg/L}$) was negligible (Figure 8b). By contrast, the OTC degradation was significantly reduced by the organic compounds present in the secondary effluent ($\text{pH} = 7.2$, $[\text{DOC}]_0 = 4.71 \text{ mg/L}$, $\text{UV}_{254} = 0.100$, $\text{SUVA} = 2.12$) (Figure 8c). This is because the electron-rich moieties in the molecular structure of natural organic matter (NOM) present in the secondary effluent can be readily attacked by electrophilic radicals such as $\text{SO}_4^{\bullet-}$ and HO^\bullet [44].



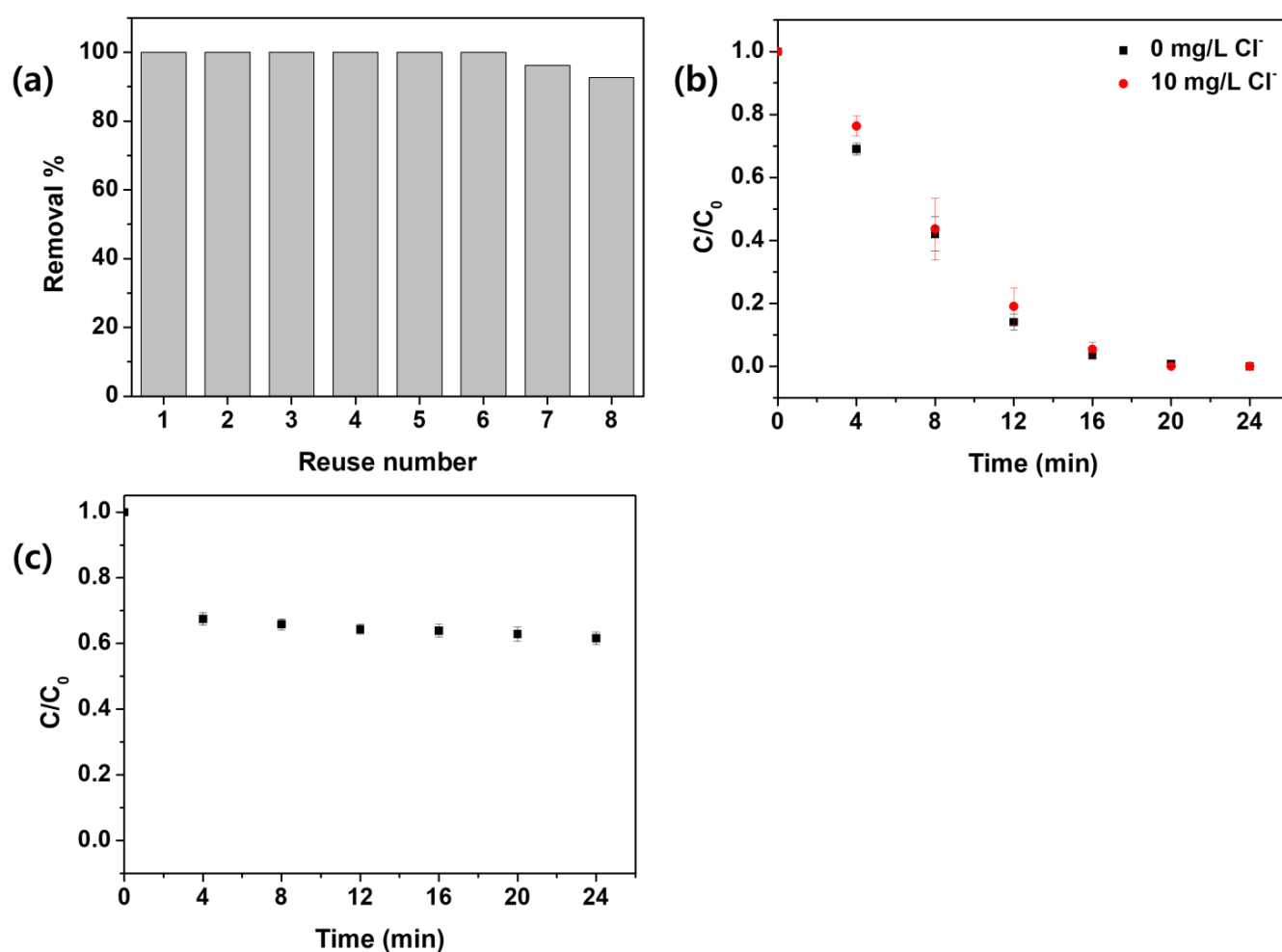


Figure 8. (a) Sequential oxytetracycline (OTC) degradation test ($[PS]_0 = 1$ mM, $[OTC]_0 = 20$ μ M, $[HWWC]_0 = 0.2$ g/L, pH = 6); (b) OTC degradation in the presence of Cl^- ($[Cl^-]_0 = 10$ mg/L); (c) Degradation kinetics of OTC by persulfate activation using HWWC in the secondary effluent (pH = 7.2, $[DOC]_0 = 4.71$ mg/L, $UV_{254} = 0.100$, $SUVA = 2.12$). PS: persulfate; HWWC: hand-warmer waste catalyst.

4. Conclusions

HWWC was successfully prepared by a simple magnetic separation method. The XRD and SEM-EDS results revealed that the HWWC consisted of a mixture of γ - Fe_2O_3 and α - Fe_2O_3 . The magnetic saturation of HWWC was sufficient to be separated by conventional magnets, which can facilitate their application for water treatment. The control experiment showed that OTC was removed by the generated radical species when both HWWC and PS were present. $SO_4^{\bullet-}$ was the dominant oxidizing species in the OTC degradation by persulfate activation using HWWC catalyst. Influencing parameters such as HWWC dose, PS concentration, and solution pH were evaluated, and the degradation efficiency of OTC increased with increasing HWWC dose and PS concentration, and the optimal pH values for OTC degradation were 3 and 4. In addition, the HWWC degraded OTC after eight repeat experiments with great stability. Degradation efficiency was significantly affected by NOM present in the secondary effluent, while the effect of chloride ions was negligible. Overall, these results suggest that PS activation using magnetic Fe_2O_3 catalysts derived from hand-warmer waste could be an effective alternative for removing OTC and other recalcitrant organic compounds in water.

Author Contributions: Conceptualization, Y.-J.L. and C.-G.L.; methodology, Y.-J.L.; validation, Y.-J.L.; formal analysis, Y.-J.L.; writing—original draft preparation, Y.-J.L.; writing—review and editing, C.-G.L., S.-J.P. and E.H.J.; visualization, Y.-J.L.; supervision, C.-G.L., S.-J.P. and E.H.J.; funding acquisition, E.H.J. All authors have read and agreed to the published version of the manuscript.

Funding: This work was conducted with the support of the Cooperative Research Program for Agriculture Science and Technology Development (Project No. PJ01571602), Rural Development Administration, Korea.

Institutional Review Board Statement: Not applicable.

Informed Consent Statement: Not applicable.

Conflicts of Interest: The authors declare no conflict of interest.

References

1. Liu, D.; Li, M.; Li, X.; Ren, F.; Sun, P.; Zhou, L. Core-shell Zn/Co MOFs derived Co₃O₄/CNTs as an efficient magnetic heterogeneous catalyst for persulfate activation and oxytetracycline degradation. *Chem. Eng. J.* **2020**, *387*, 124008. [\[CrossRef\]](#)
2. Baquero, F.; Martínez, J.L.; Canton, R. Antibiotics and antibiotic resistance in water environments. *Curr. Opin. Biotechnol.* **2008**, *19*, 260–265. [\[CrossRef\]](#)
3. Wang, L.; Yang, H.; Zhang, C.; Mo, Y.; Lu, X. Determination of oxytetracycline, tetracycline and chloramphenicol antibiotics in animal feeds using subcritical water extraction and high performance liquid chromatography. *Anal. Chim. Acta* **2008**, *619*, 54–58. [\[CrossRef\]](#)
4. Uslu, M.O.; Balcioglu, I.A. Simultaneous removal of oxytetracycline and sulfamethazine antibacterials from animal waste by chemical oxidation processes. *J. Agric. Food Chem.* **2009**, *57*, 11284–11291. [\[CrossRef\]](#) [\[PubMed\]](#)
5. Liu, Y.; He, X.; Fu, Y.; Dionysiou, D.D. Kinetics and mechanism investigation on the destruction of oxytetracycline by UV-254nm activation of persulfate. *J. Hazard. Mater.* **2016**, *305*, 229–239. [\[CrossRef\]](#)
6. Kemper, N. Veterinary antibiotics in the aquatic and terrestrial environment. *Ecol. Indic.* **2008**, *8*, 1–13. [\[CrossRef\]](#)
7. Sarmah, A.K.; Meyer, M.T.; Boxall, A.B. A global perspective on the use, sales, exposure pathways, occurrence, fate and effects of veterinary antibiotics (VAs) in the environment. *Chemosphere* **2006**, *65*, 725–759. [\[CrossRef\]](#)
8. Kummerer, K. Antibiotics in the aquatic environment—A review—Part I. *Chemosphere* **2009**, *75*, 417–434. [\[CrossRef\]](#)
9. Zheng, S.; Qiu, X.; Chen, B.; Yu, X.; Liu, Z.; Zhong, G.; Li, H.; Chen, M.; Sun, G.; Huang, H.; et al. Antibiotics pollution in Jiulong River estuary: Source, distribution and bacterial resistance. *Chemosphere* **2011**, *84*, 1677–1685. [\[CrossRef\]](#)
10. Li, B.; Zhang, T. Mass flows and removal of antibiotics in two municipal wastewater treatment plants. *Chemosphere* **2011**, *83*, 1284–1289. [\[CrossRef\]](#)
11. Li, W.; Shi, Y.; Gao, L.; Liu, J.; Cai, Y. Occurrence and removal of antibiotics in a municipal wastewater reclamation plant in Beijing, China. *Chemosphere* **2013**, *92*, 435–444. [\[CrossRef\]](#)
12. Xu, J.; Xu, Y.; Wang, H.; Guo, C.; Qiu, H.; He, Y.; Zhang, Y.; Li, X.; Meng, W. Occurrence of antibiotics and antibiotic resistance genes in a sewage treatment plant and its effluent-receiving river. *Chemosphere* **2015**, *119*, 1379–1385. [\[CrossRef\]](#)
13. Golovko, O.; Kumar, V.; Fedorova, G.; Randak, T.; Grabic, R. Seasonal changes in antibiotics, antidepressants/psychiatric drugs, antihistamines and lipid regulators in a wastewater treatment plant. *Chemosphere* **2014**, *111*, 418–426. [\[CrossRef\]](#)
14. Chen, J.; Hu, Y.; Huang, W.; Liu, Y.; Tang, M.; Zhang, L.; Sun, J. Biodegradation of oxytetracycline and electricity generation in microbial fuel cell with in situ dual graphene modified bioelectrode. *Bioresour. Technol.* **2018**, *270*, 482–488. [\[CrossRef\]](#)
15. Garrido-Ramírez, E.G.; Theng, B.K.G.; Mora, M.L. Clays and oxide minerals as catalysts and nanocatalysts in Fenton-like reactions—A review. *Appl. Clay Sci.* **2010**, *47*, 182–192. [\[CrossRef\]](#)
16. Feng, Y.; Wu, D.; Liao, C.; Deng, Y.; Zhang, T.; Shih, K. Red mud powders as low-cost and efficient catalysts for persulfate activation: Pathways and reusability of mineralizing sulfadiazine. *Sep. Purif. Technol.* **2016**, *167*, 136–145. [\[CrossRef\]](#)
17. Liang, C.J.; Bruell, C.J.; Marley, M.C.; Sperry, K.L. Thermally Activated Persulfate Oxidation of Trichloroethylene (TCE) and 1,1,1-Trichloroethane (TCA) in Aqueous Systems and Soil Slurries. *Soil Sediment Contam. Int. J.* **2010**, *12*, 207–228. [\[CrossRef\]](#)
18. Zhang, T.; Chen, Y.; Wang, Y.; Le Roux, J.; Yang, Y.; Croue, J.P. Efficient peroxydisulfate activation process not relying on sulfate radical generation for water pollutant degradation. *Environ. Sci. Technol.* **2014**, *48*, 5868–5875. [\[CrossRef\]](#) [\[PubMed\]](#)
19. Abu Amr, S.S.; Aziz, H.A.; Adlan, M.N. Optimization of stabilized leachate treatment using ozone/persulfate in the advanced oxidation process. *Waste Manag.* **2013**, *33*, 1434–1441. [\[CrossRef\]](#)
20. Peng, L.; Deng, D.; Guan, M.; Fang, X.; Zhu, Q. Remediation HCHs POPs-contaminated soil by activated persulfate technologies: Feasibility, impact of activation methods and mechanistic implications. *Sep. Purif. Technol.* **2015**, *150*, 215–222. [\[CrossRef\]](#)
21. Liu, C.S.; Shih, K.; Sun, C.X.; Wang, F. Oxidative degradation of propachlor by ferrous and copper ion activated persulfate. *Sci. Total Environ.* **2012**, *416*, 507–512. [\[CrossRef\]](#)
22. Teel, A.L.; Ahmad, M.; Watts, R.J. Persulfate activation by naturally occurring trace minerals. *J. Hazard. Mater.* **2011**, *196*, 153–159. [\[CrossRef\]](#)
23. Fang, G.-D.; Dionysiou, D.D.; Al-Abed, S.R.; Zhou, D.-M. Superoxide radical driving the activation of persulfate by magnetite nanoparticles: Implications for the degradation of PCBs. *Appl. Catal. B: Environ.* **2013**, *129*, 325–332. [\[CrossRef\]](#)

24. Ioannidi, A.; Oulego, P.; Collado, S.; Petala, A.; Arniella, V.; Frontistis, Z.; Angelopoulos, G.N.; Diaz, M.; Mantzavinos, D. Persulfate activation by modified red mud for the oxidation of antibiotic sulfamethoxazole in water. *J. Environ. Manag.* **2020**, *270*, 110820. [\[CrossRef\]](#) [\[PubMed\]](#)
25. Naim, S.; Ghauch, A. Ranitidine abatement in chemically activated persulfate systems: Assessment of industrial iron waste for sustainable applications. *Chem. Eng. J.* **2016**, *288*, 276–288. [\[CrossRef\]](#)
26. Lian, J.-Z.; Tsai, C.-T.; Chang, S.-H.; Lin, N.-H.; Hsieh, Y.-H. Iron waste as an effective depend on TiO₂ for photocatalytic degradation of dye waste water. *Optik* **2017**, *140*, 197–204. [\[CrossRef\]](#)
27. Yu, Y.; Paul Chen, J. Key factors for optimum performance in phosphate removal from contaminated water by a Fe-Mg-La tri-metal composite sorbent. *J. Colloid. Interface Sci.* **2015**, *445*, 303–311. [\[CrossRef\]](#)
28. Qiu, J.; Yang, R.; Li, M.; Jiang, N. Preparation and characterization of porous ultrafine Fe₂O₃ particles. *Mater. Res. Bull.* **2005**, *40*, 1968–1975. [\[CrossRef\]](#)
29. Molodtsova, T.; Gorshenkov, M.; Saliev, A.; Vanyushin, V.; Goncharov, I.; Smirnova, N. One-step synthesis of γ -Fe₂O₃/Fe₃O₄ nanocomposite for sensitive electrochemical detection of hydrogen peroxide. *Electrochim. Acta* **2021**, *370*, 137723. [\[CrossRef\]](#)
30. Khoshnam, M.; Salimijazi, H. Synthesis and characterization of magnetic-photocatalytic Fe₃O₄/SiO₂/ α -Fe₂O₃ nano core-shell. *Surf. Interfaces* **2021**, *26*, 101322. [\[CrossRef\]](#)
31. Chu, J.-H.; Kang, J.-K.; Park, S.-J.; Lee, C.-G. Application of magnetic biochar derived from food waste in heterogeneous sono-Fenton-like process for removal of organic dyes from aqueous solution. *J. Water Process Eng.* **2020**, *37*, 101455. [\[CrossRef\]](#)
32. Chu, J.-H.; Kang, J.-K.; Park, S.-J.; Lee, C.-G. Enhanced sonocatalytic degradation of bisphenol A with a magnetically recoverable biochar composite using rice husk and rice bran as substrate. *J. Environ. Chem. Eng.* **2021**, *9*, 105284. [\[CrossRef\]](#)
33. Zouanti, M.; Bezzina, M.; Dhib, R. Experimental study of degradation and biodegradability of oxytetracycline antibiotic in aqueous solution using Fenton process. *Environ. Eng. Res.* **2019**, *25*, 316–323. [\[CrossRef\]](#)
34. Ma, Q.; Zhang, X.; Guo, R.; Zhang, H.; Cheng, Q.; Xie, M.; Cheng, X. Persulfate activation by magnetic γ -Fe₂O₃/Mn₃O₄ nanocomposites for degradation of organic pollutants. *Sep. Purif. Technol.* **2019**, *210*, 335–342. [\[CrossRef\]](#)
35. Guan, Y.H.; Ma, J.; Ren, Y.M.; Liu, Y.L.; Xiao, J.Y.; Lin, L.Q.; Zhang, C. Efficient degradation of atrazine by magnetic porous copper ferrite catalyzed peroxymonosulfate oxidation via the formation of hydroxyl and sulfate radicals. *Water Res.* **2013**, *47*, 5431–5438. [\[CrossRef\]](#)
36. Pham, A.N.; Xing, G.; Miller, C.J.; Waite, T.D. Fenton-like copper redox chemistry revisited: Hydrogen peroxide and superoxide mediation of copper-catalyzed oxidant production. *J. Catal.* **2013**, *301*, 54–64. [\[CrossRef\]](#)
37. Liang, H.-Y.; Zhang, Y.-Q.; Huang, S.-B.; Hussain, I. Oxidative degradation of p-chloroaniline by copper oxidate activated persulfate. *Chem. Eng. J.* **2013**, *218*, 384–391. [\[CrossRef\]](#)
38. Norzaee, S.; Taghavi, M.; Djahed, B.; Kord Mostafapour, F. Degradation of Penicillin G by heat activated persulfate in aqueous solution. *J. Environ. Manag.* **2018**, *215*, 316–323. [\[CrossRef\]](#)
39. Liang, C.; Lee, I.L. In situ iron activated persulfate oxidative fluid sparging treatment of TCE contamination—a proof of concept study. *J. Contam. Hydrol.* **2008**, *100*, 91–100. [\[CrossRef\]](#)
40. Chen, Y.; Yan, J.; Ouyang, D.; Qian, L.; Han, L.; Chen, M. Heterogeneously catalyzed persulfate by CuMgFe layered double oxide for the degradation of phenol. *Appl. Catal. A: Gen.* **2017**, *538*, 19–26. [\[CrossRef\]](#)
41. Long, M.; Brame, J.; Qin, F.; Bao, J.; Li, Q.; Alvarez, P.J. Phosphate Changes Effect of Humic Acids on TiO₂ Photocatalysis: From Inhibition to Mitigation of Electron-Hole Recombination. *Environ. Sci. Technol.* **2017**, *51*, 514–521. [\[CrossRef\]](#) [\[PubMed\]](#)
42. Li, Z.; Chen, Z.; Xiang, Y.; Ling, L.; Fang, J.; Shang, C.; Dionysiou, D.D. Bromate formation in bromide-containing water through the cobalt-mediated activation of peroxymonosulfate. *Water Res.* **2015**, *83*, 132–140. [\[CrossRef\]](#) [\[PubMed\]](#)
43. Chu, J.-H.; Kang, J.-K.; Park, S.-J.; Lee, C.-G. Ultrasound-activated peroxydisulfate process with copper film to remove bisphenol A: Operational parameter impact and back propagation-artificial neural network modeling. *J. Water Process Eng.* **2021**, *44*, 102326. [\[CrossRef\]](#)
44. Ma, J.; Yang, Y.; Jiang, X.; Xie, Z.; Li, X.; Chen, C.; Chen, H. Impacts of inorganic anions and natural organic matter on thermally activated persulfate oxidation of BTEX in water. *Chemosphere* **2018**, *190*, 296–306. [\[CrossRef\]](#)